Elastic properties of $Mg_{(1-x)}Al_xB_2$ from first principles theory



2004 J. Phys.: Condens. Matter 16 5241

(http://iopscience.iop.org/0953-8984/16/29/015)

INSTITUTE OF PHYSICS PUBLISHING JOURNAL OF PHYSICS: CONDENSED MATTER

J. Phys.: Condens. Matter **16** (2004) 5241–5250 PII: S0953-8984(04)80743-4

# Elastic properties of $Mg_{(1-x)}Al_xB_2$ from first principles theory

**P Souvatzis, J M Osorio-Guillén, R Ahuja, A Grechnev and O Eriksson**

Department of Physics, Uppsala University, Box 530, SE-75121, Uppsala, Sweden

Received 7 May 2004
Published 9 July 2004
Online at stacks.iop.org/JPhysCM/16/5241
doi:10.1088/0953-8984/16/29/015

**Abstract**

Elastic properties of $Mg_{(1-x)}Al_xB_2$ have been studied from first principles. The elastic constants ($c_{11}$, $c_{12}$, $c_{13}$, $c_{33}$ and $c_{55}$) have been calculated, in the regime of $x = 0$ to 0.25. From these calculations the ratio between the bulk modulus and shear modulus (B/G) as well as the ratio between the two directional bulk moduli ($B_a/B_c$) have been evaluated. Our calculations show that the ratio $B_a/B_c$ decreases monotonically as the aluminium content is increased, whereas the ratio B/G is well below the empirical ductility limit, 1.75, for all concentrations. In addition, we analyse the electronic structure and the nature of the chemical bonding, using the balanced crystal orbital overlap population (BCOOP) (Grechnev *et al* 2003 *J. Phys.: Condens. Matter* **15** 7751) and the charge densities. Our analysis suggests that, while aluminium doping decreases the elastic anisotropy of $MgB_2$ in the $a$ and $c$ directions, it will not change the brittle behaviour of the material considerably.

(Some figures in this article are in colour only in the electronic version)

## 1. Introduction

The discovery of superconductivity in $MgB_2$ [2] has inspired large parts of the material science community to undertake experimental and theoretical studies of this compound. The primary motivation of this extensive interest in $MgB_2$ arises of course from the fact that it has a critical superconducting temperature [2] of 39 K which is unexpectedly high, compared with other inter-metallic compounds. Several experimental and theoretical results from studies of $MgB_2$ have been reported. In particular theoretical investigations of the mechanisms behind the superconductive properties have been made by Choi *et al* [3]. The pressure dependence of the superconducting transition temperature, $T_c$, has been investigated by Saito *et al* [4] and Monteverde *et al* [5]. Tampieri *et al* [8] showed that copper doping in $MgB_2$ results in a decrease in $T_c$, similar to that produced by aluminium doping reported in [9].

Parallel with these studies there has been a considerable development in the techniques for manufacturing $MgB_2$ wires. The main technique used is the powder in tube process

  

(PIT process) [6], which has been successfully used to produce up to 100 m long wires [7]. However, the manufacturing of these long wires is still a very delicate matter, due to the very low critical strain of about 0.1% [7]. Despite this limitation, only a few of the studies made on $MgB_2$ are concerned with mechanical properties, especially those investigations which are undertaken within the framework of theory. However, some studies have indeed involved *ab initio* calculations of the elastic properties [10, 11]. These theoretical works all come to the conclusion that $MgB_2$ is elastically anisotropic, i.e. the compressibilities in the $a$ and $b$ directions differ by a factor of 1.82 [10] to 2.39 [11]. This is confirmed by the experimental data on the previously mentioned compressibilities, which reveals differences of a factor of 1.67 [12] to 1.88 [13]. Since the elastic anisotropy is known, at least on empirical grounds, to correlate to the brittleness of a material [14], these theoretical results indicate that $MgB_2$ is a fairly brittle material, in agreement with observations. This unfortunate property limits the practical use of $MgB_2$, especially the manufacturing of wires, and thus underlines the importance of continued investigations of the elastic behaviour of $MgB_2$. In the current paper we have, from an *ab initio* point of view, studied how aluminium doping influences the elastic properties of $MgB_2$ and how the brittleness of the material is expected to change with alloying. It should be noted that the structural properties of Al doped $MgB_2$ have been studied experimentally and that for certain Al concentrations (i.e. 25%) a superstructure was observed [15]. In addition the chemical bonding of $Mg_{(1-x)}Al_xB_2$ is discussed, based on an analysis of the charge density, the electronic structure and the newly introduced balanced crystal orbital overlap population (BCOOP) [1].

## 2. Calculational details

### *2.1. Calculation of elastic properties*

The elastic properties were calculated, with the use of density functional theory in the generalized gradient approximation. The Kohn–Sham equations were solved by the full-potential linear muffin-tin orbital (FP-LMTO) method [16–18]. The muffin-tin orbitals were expanded in a series of spherical harmonics (with a cut-off $l_{\max} = 6$), within the muffin-tin spheres. Fourier series were used in expanding the density and potential in the interstitial regions. A so called double basis set was used, involving two tails. In order to speed up the convergence, a Gaussian broadening of 20 mRyd was applied to each eigenvalue. In these calculations 845 **k** points have been used in the irreducible part of the BZ, to guarantee the energy resolution needed. The doping of aluminium into the system was introduced within the framework of the virtual crystal approximation (VCA). In order to check the validity of this approximation, both the VCA and the supercell method were used to obtain the elastic constants for $Mg_{0.75}Al_{0.25}B_2$ (table 1). Concerning the specific details on the strains used to obtain the different elastic constants we refer to the paper of Ravindran *et al* [10].

### *2.2. Calculation of the BCOOP*

To investigate the chemical bonding situation in $Mg_{(1-x)}Al_xB_2$, the balanced crystal orbital overlap population (BCOOP) [1] has been calculated for Al concentrations ranging from $x = 0.0$ to 0.25. This method has its strength in identifying covalent chemical bonds and which components of these bonds that are bonding and which are anti-bonding. The method of BCOOP is based on the same idea as the crystal orbital overlap population (COOP) method by Hughbanks and Hoffmann [19]. The COOP is defined as an orbital-population weighted

**Table 1.** The five independent elastic constants (in GPa) of $MgB_2$ calculated for different concentrations of aluminium using VCA.

| $x$ | $c_{11}$ | $c_{12}$ | $c_{13}$ | $c_{33}$ | $c_{55}$ |
|---|---|---|---|---|---|
| 0.00 | 435 | 47 | 36 | 263 | 72 |
| 0.02 | 438 | 48 | 36 | 266 | 70 |
| 0.05 | 443 | 49 | 35 | 272 | 68 |
| 0.07 | 445 | 49 | 33 | 277 | 68 |
| 0.10 | 450 | 50 | 33 | 281 | 69 |
| 0.12 | 455 | 50 | 33 | 285 | 70 |
| 0.15 | 457 | 50 | 33 | 288 | 75 |
| 0.17 | 460 | 51 | 32 | 290 | 73 |
| 0.20 | 464 | 52 | 31 | 295 | 76 |
| 0.22 | 467 | 53 | 32 | 299 | 75 |
| 0.25 | 471 | 53 | 32 | 303 | 70 |
| 0.25[a] | 458 | 66 | 26 | 301 | 69 |

[a] Supercell calculation.

density of states:

$$\mathrm{COOP}_{ij}(\epsilon) = \sum_n \int_{\mathrm{BZ}} \frac{\mathrm{d}\mathbf{k}}{(2\pi)^3}\, \delta(\epsilon - \epsilon_n(\mathbf{k})) c_i^* c_j S_{ij} \tag{1}$$

where

$$S_{ij} = \langle e_i | e_j \rangle \tag{2}$$

is the overlap matrix between the basis functions $|e_i\rangle$ used to expand the eigenvector

$$|\psi_n(\mathbf{k})\rangle = \sum_i c_i |e_i\rangle, \tag{3}$$

corresponding to the eigenvalue $\epsilon_n(\mathbf{k})$. Furthermore, the basis set $\{|e_i\rangle\}$ should consist of atomic-like orbitals, localized on the different types of atom in the unit cell, in order for the $\mathrm{COOP}_{ij}(\epsilon)$ to give meaningful information about the bonding situation in the material. The $\mathrm{COOP}_{ij}(\epsilon)$ is an energy resolved measure of the bonding between the orbitals $|e_i\rangle$ and $|e_j\rangle$. This measure will have positive and negative values corresponding to bonding and anti-bonding states, respectively. Unfortunately, the $\mathrm{COOP}_{ij}(\epsilon)$ is a basis set dependent quantity [1], and in the limit of nearly linear dependent basis set this method overestimates the anti-bonding character. However, the BCOOP greatly suppresses the basis set dependence and treats the bonding and anti-bonding states on more or less equal terms. The BCOOP of Grechnev *et al* [1] is given by

$$\mathrm{BCOOP}_{ij}(\epsilon) = \sum_n \int_{\mathrm{BZ}} \frac{\mathrm{d}\mathbf{k}}{(2\pi)^3}\, \delta(\epsilon - \epsilon_n(\mathbf{k})) \frac{c_i^* c_j S_{ij}}{\sum_\alpha \sum_{i',j' \in A(\alpha)} c_{i'}^* c_{j'} S_{i'j'}} \tag{4}$$

where $A(\alpha)$ is the subset of eigenvectors corresponding to the same type of atom and orbital. In the calculations presented here we have implemented the BCOOP in the FP-LMTO method. This means that the basis sets used consist of muffin-tin orbitals, and that the sum $\sum_{i',j' \in A(\alpha)}$ is equivalent to the sum over all tails and magnetic quantum numbers, since we have only used one basis set per atom type. In the BCOOP calculations 1500 $\mathbf{k}$ points were used in the irreducible BZ, and in the last iteration the linear tetrahedron method was implemented, instead of the previously mentioned Gaussian smearing.

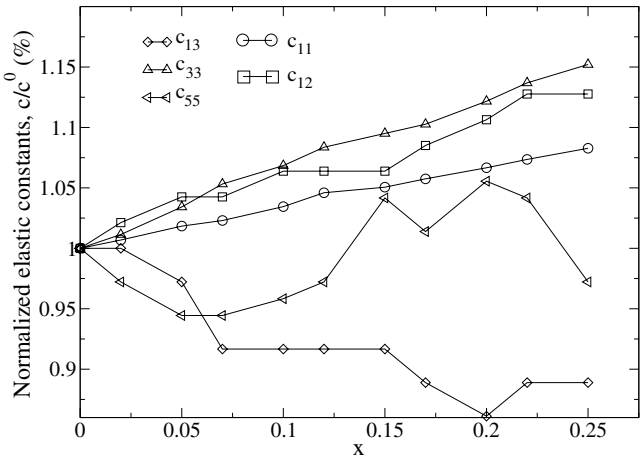


**Figure 1.** The elastic constants (normalized with their respective values at zero concentration of Al) for different dopings of aluminium.

**Table 2.** The experimental and theoretical crystallographic lattice parameters, $B_a/B_c$-ratio, bulk modulus and its pressure derivative for $MgB_2$.

| | Expt | Theor. |
|---|---|---|
| a (Å) | 3.086[a] | 3.088 |
| $c/a$ | 1.142[a] | 1.143 |
| $B_a/B_c$ | 1.67[c] 1.88[d] | 1.81 |
| B (GPa) | 151[b] | 152 |
| B′ (GPa) | 4.0[b] | 3.65 |

[a] Reference [2].
[b] Reference [21].
[c] Reference [12].
[d] Reference [13].

## 3. Results

### *3.1. Elastic properties*

The calculated elastic properties are listed in table 1, for all alloying concentrations. It should be noticed that for pure $MgB_2$ the results of table 1 are in good agreement with previous calculations [10, 11]. Unfortunately, there are to our knowledge no experimental data reported for $Mg_{(1-x)}Al_xB_2$ and our results serve as a theoretical prediction. At the bottom of table 1 the elastic constants for the aluminium content of 25% are presented for the VCA and the supercell calculations, and we may notice that these two approximations give very similar results. A comparison that can be made with experiment includes the equilibrium lattice constant, bulk modulus and its pressure derivative (table 2), and here the agreement is good.

In order to illustrate the changes in the different elastic constants due to aluminium doping, we show in figure 1 the calculated values of $c_{ij}$ normalized to the value given for pure $MgB_2$. It can be seen that most of the elastic constants increase with Al doping, with the exception of $c_{13}$, that decreases, and $c_{55}$, that behaves irregularly: initially decreasing, then increasing and finally decreasing again. This suggests an enhanced elastic anisotropy when Al replaces some

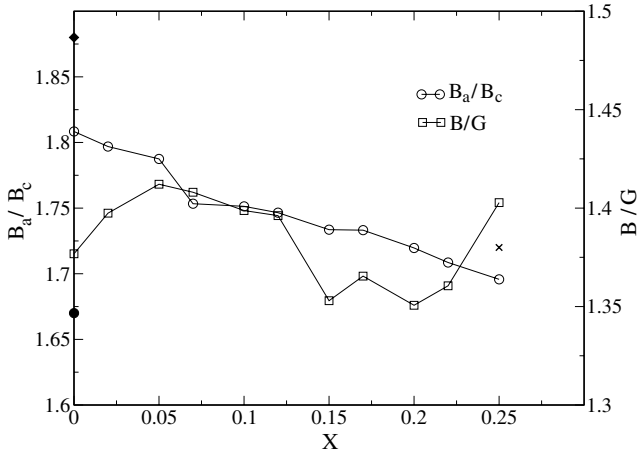


**Figure 2.** Calculated ratios between the two directional bulk moduli $B_a/B_c$, together with the ratios between the bulk and shear moduli, for different aluminium dopings. The cross corresponds to the supercell calculation of $B_a/B_c$. The filled circle and diamond correspond to the experimental values of $B_a/B_c$ found in [12] and [13].

of the B atoms. However, when calculating the ratio of the compressibilities in the $a$- and $c$-directions

$$B_a = \frac{\Lambda}{2+\beta} \tag{5}$$

$$B_c = \frac{B_a}{\beta} \tag{6}$$

where

$$\Lambda = 2(c_{11} + c_{12} + 2c_{13}\beta) + c_{33}\beta^2 \tag{7}$$

$$\beta = \frac{c_{11} + c_{12} - 2c_{13}}{c_{33} - c_{13}} \tag{8}$$

we notice that the situation is quite different. With increasing Al concentration this ratio actually decreases. Since the ratio $B_a/B_c$ is approximately proportional to the ratio between the largest elastic constants $c_{11}$ and $c_{33}$, the decrease of the elastic anisotropy can be directly traced down to the behaviour of these constants (figure 1).

What is also predicted, in figure 2, is that initially, i.e. for an aluminium concentration of <5%, the ratio between bulk and shear moduli, B/G, increases monotonically. The ratio between these particular materials constants is important, since on empirical grounds it has been argued that a material should be ductile if this ratio is larger than 1.75 and brittle if the ratio is less than 1.75 [14]. Since the ratio B/G stays well below this ductility limit, our results suggest that no great improvement of the ductile properties could be expected by forming $Mg_{(1-x)}Al_xB_2$. However since in practical applications $MgB_2$ is not single crystalline, the ductility also crucially depends on the size of the grains and the nature of the grain boundaries and their ability to stop and deflect cracks. Thus in order to draw any strong conclusions on how the ductility of $MgB_2$ is affected by the introduction of Al, further investigations have to be made. Several studies have been made on the effect that grains and their boundaries have on the ductility of a material; here we refer to the work of Shenoy *et al* [20].

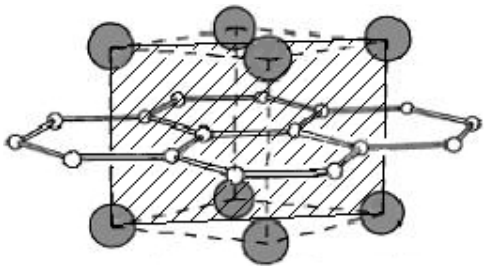

**Figure 3.** The crystal structure of $MgB_2$. The shaded plane, orthogonal to both the magnesium layer (grey circles) and the boron layer (white circles), corresponds to the section in which the charge density of figure 6 has been calculated.

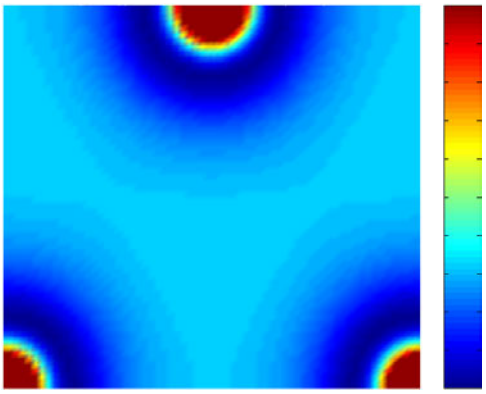

**Figure 4.** The charge density for the magnesium layer, in $MgB_2$.

### *3.2. The electronic structure and chemical bonding of $MgB_2$*

The chemical bonding in $MgB_2$ is somewhat complex, and previous studies [10, 11] have agreed that the B–B inplane bonding is of strong covalent character; the Mg–B interplane bonding and the inplane Mg–Mg bonding have more or less ionic and metallic features respectively. These conclusions have been based on the studies of the crystal overlap Hamiltonian population [10], the valence charge density and the electron localization function [11]. In this work we have studied the nature of the different bonds of $Mg_{1-x}Al_xB_2$, by studying the charge density, electronic structure and BCOOP. The charge density and the BCOOP between nearest neighbours have been calculated in three different planes (figure 3) of the $MgB_2$ crystal. In figure 4, we show the charge density of $MgB_2$ in the Mg layer. A more or less featureless distribution of charge can be seen, which suggests that the bonding between these atoms is of metallic character. The charge distribution in the boron plane (figure 5), with its high concentration of charge between the boron atoms, shows a bonding with strong covalent features. Finally, for a plane involving both Mg and B atoms (figure 6) we note again the strong covalent bond between B atoms, but no strong features between Mg and B atoms, ruling out a covalent bond between Mg and B. In fact there is a rather pronounced ionic component to this bond. This component may be quantified by calculating, for the same magnesium muffin-tin radius, the difference between the number of electrons inside the magnesium muffin-tins of pure magnesium (using the experimental equilibrium volume of magnesium) and of $MgB_2$.

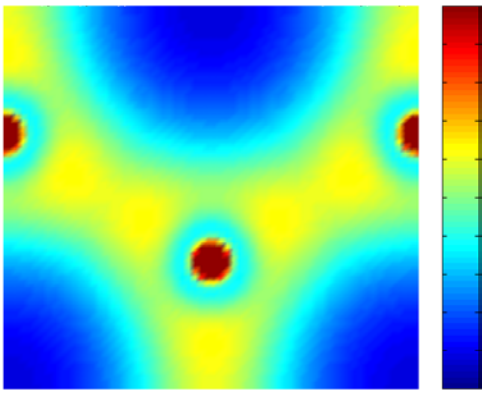

**Figure 5.** The charge density for the boron layer, in $MgB_2$.

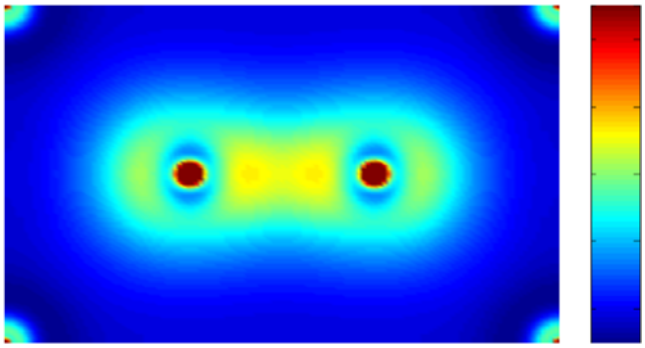

**Figure 6.** The charge density for the section through both magnesium and boron atoms, in $MgB_2$.

This estimate predicts that around 0.5 electrons leave the vicinity of the Mg atoms when we go from pure Mg to $MgB_2$.

Aside from discussing the bonding situation in $MgB_2$ qualitatively, we have also attempted to give some quantitative information regarding the bonding. The calculated BCOOP (figure 7) clearly identifies for the B–B bonding a positive region at lower energies and a negative region at higher energies. This is a typical feature of covalent bonds, with binding states (positive BCOOP) being separated from anti-bonding (negative BCOOP). When analysing the BCOOP it is also useful to glance at the electronic structure as given by the density of states (DOS), in figure 8. Our calculations reveal that the biggest contribution to the bonding between the boron atoms comes from the p–p orbital overlap. It can also be seen that the position of the Fermi level ($E_F$) is such that almost all bonding states are filled whereas the anti-bonding states are empty. Figure 8 also shows that the boron s electrons, participate more weakly in the B–B bonding, giving a bonding contribution when overlapping with the boron p orbitals, whereas the overlap with neighbouring boron s orbitals is composed of both bonding and anti-bonding states.

The upper panel of figure 7 shows the BCOOP between Mg and B. Here the BCOOP does not reveal a clear picture of strong covalent bonds, since we cannot identify the two typical regions for covalency: one at low energies being positive and one at higher energies being negative. Instead the BCOOP is negative at low energies, then becomes positive and at high energies it is negative again. We can conclude from this that the Mg–B bond is not

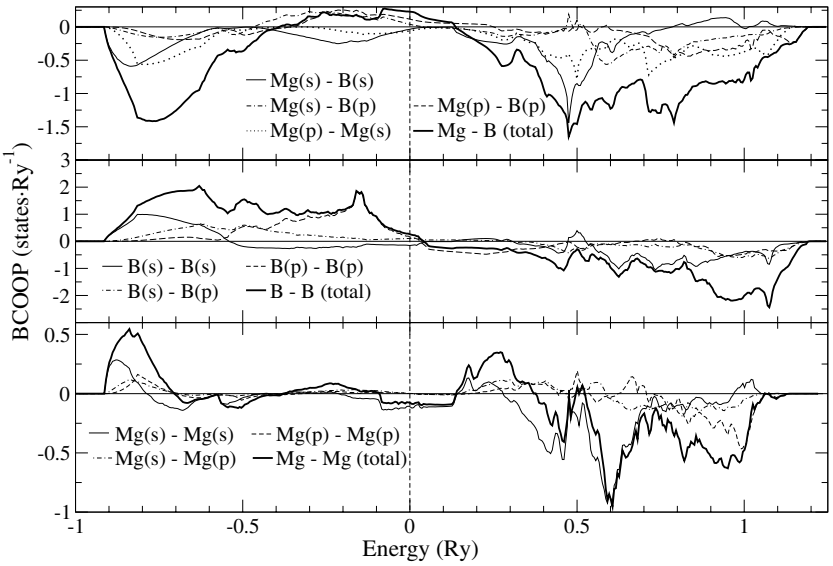


**Figure 7.** The BCOOP between magnesium and boron, the BCOOP between boron and boron and the BCOOP between magnesium and magnesium, in $MgB_2$. The Fermi level is at zero energy.

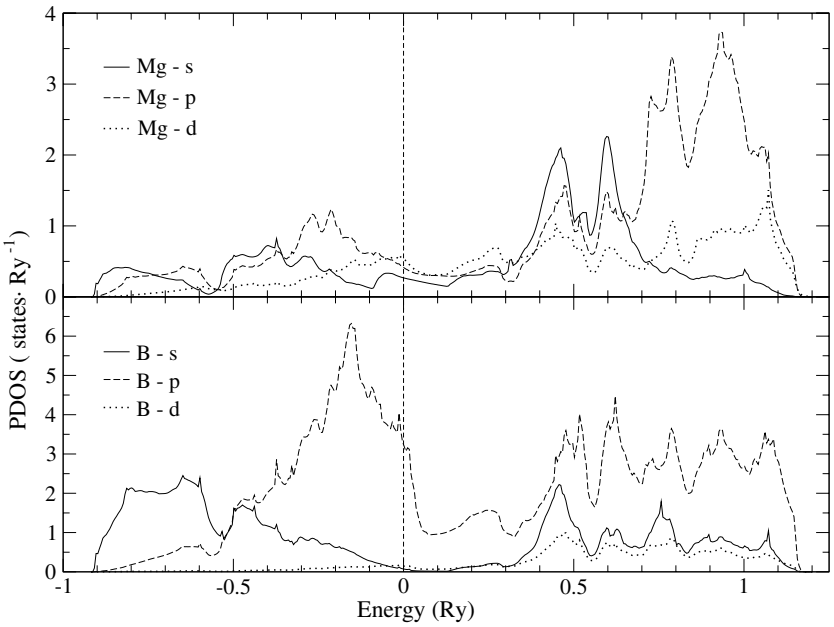


**Figure 8.** The partial density of states for magnesium and boron, in $MgB_2$. The Fermi level is at zero energy.

particularly covalent, but from the BCOOP alone we cannot conclude whether the Mg–B bond is ionic or metallic. However, from the discussion around the charge density above, we drew the conclusion that this bond has a strong ionic component, and the BCOOP of figure 7 is consistent with this picture.

The lower panel of figure 7 shows the BCOOP between the Mg atoms. Here the states of lowest energy display a clear bonding character, while the high energy states (above 0.5 Ryd) are attributed as anti-bonding. However, the BCOOP cannot be divided into unique bonding and anti-bonding energy domains, as in the B–B case. This suggest that even though the BCOOP in the Mg–Mg case displays some covalent features, it does not justify the classification of the bond as being covalent, at least not purely covalent. This conclusion is also supported by the previous discussion around the charge density, where we concluded that the bond had a more or less metallic character. Hence, the BCOOP of figure 7, together with the charge density of figure 4, implies that the Mg–Mg bonding has a strong metallic character with some smaller covalent features.

The BCOOP in the case of Al doping was also calculated in connection with the 0.25% supercell calculation. Here the BCOOPs between the different types of Mg and B atom appearing in the supercell showed no difference in character compared to the BCOOPs calculated in the undoped case. The additional BCOOPs calculated to investigate the character of the Mg–Al bond and the B–Al bond showed that these bonds were of metallic and ionic character, respectively.

## 4. Summary

The calculations presented in this study have first of all shown that $MgB_2$ is elastically anisotropic, and that the bonding situation in the material is a mixture between covalent, metallic and ionic bonding. Furthermore, the BCOOP has been utilized as a measure of the bonding character, proving to be a useful complement to the information given by the charge density analysis.

The most conspicuous finding made in this study was that electron doping by introducing Al into the system might be used to decrease the elastic anisotropy of $MgB_2$, which could be used to make the material more ductile. However, the ratio between the bulk and shear moduli, B/G, is for all Al concentrations below 1.75, i.e. below the phenomenological criterion for ductility [14]. Also, for concentrations of Al above 0.25% the superconductive properties almost completely vanish [9, 22], suggesting that elements other than Al should be used in the method of electron doping, in order for this method to be an effective remedy to the brittle behaviour of $MgB_2$.

## Acknowledgments

We are grateful to the Strategic Foundation for Research (SSF), the Swedish Research Council (VR), the Swedish National Supercomputer Center (NSC), the Center for Dynamical Processes at Uppsala University and the Göran Gustafsson foundation for support.

## References

[1] Grechnev A, Ahuja R and Eriksson O 2003 *J. Phys.: Condens. Matter* **15** 7751
[2] Nagamatsu J, Nakagawa N, Muranaka T and Zenitani Y 2001 *Nature* **410** 63
[3] Choi H J, Roundy D, Sun H, Cohen M L and Louie S G 2002 *Phys. Rev.* B **66** 020513
[4] Saito E, Taknenobu T, Ito T, Iwasa Y, Prassides K and Arima T 2001 *J. Phys.: Condens. Matter* **13** L267
[5] Monteverde M, Nunez-Rgueiro M, Regan K A, Hayward M A, He T, Loureiro S M and Cava R J 2001 *Science* **292** 75
[6] Jin S, Mavoori H, Bower C and van Dover R B 2001 *Nature* **411** 563
[7] Grasso G, Malagoli A, Tumino A, Fanciulli C, Ferdeghini C, Siri A S, Laurenti A, Marabotto R and Modica M 2003 Development of $MgB_2$ superconducting tapes: present status and future perspectives *Proc. Symp. on*

*New Perspectives and Frontiers in Superconductor Development: Thin Films, Tapes and Wires, held at the European Materials Conf. (Lausanne, Switzerland, Sept. 2003)*
[8] Tampieri A, Celotti G, Spiro S, Rinaldi D, Barucca G and Caciuffo R 2002 *Solid State Commun.* **121** 497
[9] Monteverde M, Rogado N, Regan K A, Hayward M A, Khalifah P, He T, Inumaru K, Loureiro S M, Haas M K, Zandbergen H W and Cava R J 2001 *Nature* **410** 343
[10] Ravindran P, Vajeeston P, Vidya R, Kjekshus A and Fjellvåg H 2001 *Phys. Rev.* B **64** 224509
[11] Osorio-Guillén J M, Simak S I, Wang Y, Johansson B and Ahuja R 2002 *Solid State Commun.* **123** 257
[12] Jorgensen J D, Hinks D G and Short S 2001 *Phys. Rev.* B **63** 224522
[13] Goncharov A F, Struzhikin V V, Gregoryanz E, Hu J, Hemley R J, Mao H K, Lapertot G, Bud'ko S L and Canfield P C 2001 *Phys. Rev.* B **64** 100509
[14] Pugh S F 1954 *Phil. Mag.* **45** 833
[15] Xiang J Y, Zheng D N, Li J Q, Li L, Lang P L, Chen H, Dong C, Che G C, Ren Z A, Qi H H, Tian H Y, Ni Y M and Zhao Z X 2002 *Phys. Rev.* B **65** 214536
[16] Wills J M, Eriksson O and Alouani M 2000 Full-potential LMTO total energy and force calculations *Electronic Structure and Physical Properties of Solids: The Uses of the LMTO Method* ed H Dreysse (Berlin: Springer) p 148
[17] Wills J M and Cooper B R 1987 *Phys. Rev.* B **36** 3809
[18] Price D L and Cooper B R 1989 *Phys. Rev.* B **39** 4945
[19] Hughbanks T and Hoffmann R 1983 *J. Am. Chem. Soc.* **105** 3528
[20] Shenoy V B, Miller R, Tadmor E B, Phillips R and Ortiz M 1998 *Phys. Rev. Lett.* **80** 742
[21] Vogt T, Schneider G, Hriljac J A, Yang G and Abell J S 2001 *Phys. Rev.* B **63** 220505
[22] Xiang J Y, Zheng D N, Li J Q, Li S L, Wen H H and Zhao Z X 2003 *Physica* C **386** 611